Int. J. Advanced Networking and Applications
Volume: 15 Issue: 04 Pages:100-200 (2023) ISSN: 0975-0290 (Special Issue – ASCIS 2023)

Wood Surface Defect Detection Using Discrete Wavelet Transform and Deep-Net Model

Rohini A. Bhusnurmath and Shaila Doddamani *
Department of Computer Science,
Karnataka State Akkamahadevi Women's University,
Vijayapura-586108, Karnataka, India
Email: rohiniabmath@gmail.com Email:dodamanishaila@gmail.com

----------ABSTRACT----------

In the realm of the modern economy, wood structures and products hold immense significance, serving a wide array of applications. However, within production systems handling wood raw materials, numerous challenges arise. The high variability in raw materials, accompanied by a diverse range of structural flaws, presents complexities in the production processes. Verifying these flaws, whether online or offline remains a critical task, often relying on manual inspection. Yet, manual procedures not only encounter challenges and biases but also prove ineffective and misleading.

The study shows discrete wavelet analysis's effectiveness in defect detection across diverse wood types. However, accurately classifying defects becomes challenging due to the complexity of higher-level directional coefficients obtained from DWT. To address this, the proposed DWT-Deep-Net model combines CNN and RNN (LSTM). This fusion simplifies defect classification after DWT, using mean square energy from detailed coefficients, enhancing defect diagnosis across various deep learning classifiers.

In the DWT-Deep-Net model, the CNN and LSTM components work in tandem: the CNN adeptly extracts abstract features from raw subsequence data, automating this process, while the LSTM specializes in capturing long-term relationships within time series inputs. This integration allows for efficient extraction of abstract feature representations from the data, optimizing the classification process. Notably, the proposed methodology demonstrates superior classification accuracy when compared to existing state-of-the-art methods. This enhancement in accuracy underlines the effectiveness of this combined CNN-LSTM approach in addressing the challenges posed by defect classification post-DWT decomposition, offering promising results for wood defect detection.

Keywords – CNN, Deep learning - Discrete wavelet transform, Defect detection, Texture classification.

Date of Submission: 09-10-2023 Date of Acceptance: 15-Nov-203

I. INTRODUCTION

Wood stands as a valuable natural resource, but imperfections in wood products significantly diminish their market value. Wood veneers often exhibit flaws like live knots, dead knots, and cracks due to poor-quality raw materials and inefficient manufacturing techniques. These flaws in wood processing industries, especially in several developing nations, limit the utilization of raw timber supplies. Despite advancements, visual inspections by trained personnel remain predominant in assessing wood quality [1].

For wood veneer processing firms, optimizing wood utilization rates and maximizing profitability have become imperative. Rapid and accurate identification of wood defects is essential. Currently, various technologies such as Ultrasonic air-coupled technology [1], stress wave analysis [2], laser 3D technology [3], computed tomography [4], and computer vision [5] are employed to detect flaws in wood veneers. Among these, contactless ultrasonic measurement using air-coupled technology proves effective in identifying flaws based on changes in wood densities.

Wood, renowned for its sustainability, performance, and aesthetic appeal, holds substantial economic and artistic value. Eliminating wood defects during processing is vital to preserve its strength and texture. Traditional methods rely on manual identification, processing, and marking of solid-wood panels, prompting the wood industry to explore intelligent processing technologies since the early 21st century. Image processing, a cutting-edge technology in wood detection, has gained prominence [6, 7].

Key contributions:

- Utilizing DWT for Defect Detection: The research incorporates Discrete Wavelet Transform (DWT) from images to extract crucial aspects aiding in defect detection. By using different frequency components collected by DWT, it simplifies the distinction between normal and faulty areas, depicting distinctive defect characteristics.
- Ensemble Model - CNN and LSTM: Leveraging both Convolutional Neural Networks (CNN) and Long Short-Term Memory (LSTM) in an ensemble model enhances defect detection in wood textures by capitalizing on the strengths of each architecture.

Synergy of Wavelet Transform and Deep Learning: Unlike methods solely relying on image processing, this model combines the power of wavelet transform and deep learning. This fusion allows defect detection at various scales, providing a more comprehensive solution.

- Advantages over Traditional Approaches: The proposed model consistently outperforms traditional methods in wood texture defect detection, showcasing superior accuracy, precision, and recall. The CNN and LSTM ensemble exhibits marked improvement, highlighting their potential for enhanced performance.

Adaptability and Rule-free Approach: This approach offers significant advantages over traditional rule-based methods by effectively adapting to varying wood textures and detecting defects without predefined rules or extensive feature engineering.

- Trait Analysis and Model Improvement: The model captures a wide range of pertinent traits in wood textures by considering several features. This comprehensive analysis improves the model's capacity to recognize and categorize various flaws within wood datasets.

Scalable Architecture for Large Datasets: The model's architecture is designed to scale seamlessly with dataset sizes, making it suitable for accommodating increasingly large collections of wood texture images commonly encountered in industrial quality control.

- Epoch Analysis and Training Optimization: The study systematically analyzes the relationship between training accuracy and epoch ranges, providing insights for optimizing the training process in defect detection models. Findings suggest substantial accuracy improvement after 100 epochs, offering valuable insights for training optimization.

Contribution to Understanding Training Dynamics: By systematically analyzing the relationship between training accuracy and epoch ranges, this documentation aims to contribute to the broader understanding of training dynamics in deep learning models, specifically in defect detection scenarios.

- This article organizes its content as follows: The Section 2 delves into the prior research on wood identification and defect detection, exploring the application of diverse optimization techniques. The Section 3 outlines the problem statement, while the Section 4 provides a concise overview of the proposed solution for wood surface defect detection, covering pre-processing, feature selection, and ensemble methods. The Section 5 houses the results and discussions, and Section 6 presents the conclusion.

II. RELATED WORK

Mahmood et al. [8] focused on utilizing image processing to detect broken fabric pieces. Their approach employed discrete wavelet analysis to examine the homogeneity of fabric in digitized photographs. By identifying disruptions in the fabric's regular structure, their method effectively detected and precisely located fabric defects.

Bhusnurmath & Doddamani [9] have categorized 50 tree species based on bark textures using the BarkVN-50 dataset. They employed deep learning techniques, specifically VGG16 and MobileNet models through transfer learning. Results indicated that pre-trained models outperformed, demonstrating higher accuracy and efficiency.

Hiremath and Bhusnurmath [10] have proposed an efficient technique for classifying multiresolution textures by combining anisotropic diffusion with local directional binary patterns (LDBP). This method identified dominant LDBP descriptors in texture classification across four diverse texture datasets.

Gao et al. [11] have introduced the SE-ResNet18 model for wood knot defect recognition, authors utilized transfer learning, attention mechanisms, and convolutional neural networks (CNNs). The SE-ResNet18 model showcased improved accuracy by effectively enhancing pertinent features and reducing unnecessary ones.

Ping'an Sun [12] developed a multi-criteria framework and a deep learning algorithm for autonomous wood surface fault detection. By comparing various deep learning detection algorithms, the study emphasized precision and training efficiency, achieving significant improvements through iterative prototype enhancements.

Yaren et al. [13] investigated deep learning approaches for wood anomaly detection, authors compared CNN architectures (including MobileNet, SqueezeNet, GoogleNet, and ShuffleNet). Encouraging results were observed, particularly in categorizing normal and atypical wood products.

Shaoli et al. [14] introduced a classification approach using Local Binary Pattern and Local Binary Differential Excitation Pattern to distinguish mineral lines and cracks in birch wood veneer. By merging texture description models and employing histograms, their approach achieved effective defect categorization.

Xuyuan et al. [15] developed a feature extraction technique based on wavelet moments to extract wood defect features. Utilizing wavelet energy and invariant moments, their method computed modified Hu moment invariants, showcasing promising recognition results.

Sung-Wook Hwang et al. [16] focused on wood knot classification; this study utilized artificial neural networks and evaluated various feature extraction methods. Texture descriptors such as gray-level co-occurrence matrix and local binary patterns outperformed morphological categorization in wood knot classification.

MingyuGao et al. [17] proposed TL-ResNet34, a transfer learning-based deep learning model, for wood knot fault detection. This model, employing ResNet-34 as a feature extractor, significantly outperformed other methods in accuracy.

Mohsen and Amir [18] used a naive Bayes classification method, Mohsen and Amir focused on detecting holes in marbau and pine wood. Their study considered contact ultrasonic tests under various conditions, emphasizing the influence of testing variables on results.

Yang et al. [19] introduced a surface defect detection method for solid wood panels using the Single Shot MultiBox Detector algorithm (SSD), Yang et al. designed

an improved SSD model incorporating TensorFlow and ResNet for more accurate bounding box predictions.

III. PROBLEM STATEMENT

Wood industry involves the processing of various types of wood for construction, furniture, and other applications. However, the presence of defects in wood, like knots, cracks, and discolorations, these significantly affect to the quality and reliability of finished products. Detecting and classifying these defects accurately is crucial for ensuring product quality, minimizing waste, and maintaining customer satisfaction.Due to the variety of tree structure and the complexity of their surrounding structures, creating a robust defect detection technique for wood presents hurdles.Traditional techniques for detecting wood defects frequently call for the manual extraction of pertinent features, which can be time-consuming and may not fully account for all differences. Convolutional neural networks (CNNs), in particular, are among the Deep learning models autonomously acquire hierarchical features from unprocessed images, enabling them to recognize complex fault patterns without relying on manually created features.

The goal of this study is to propose a deeper network model-based approach for finding wood defects. The model Deep-Net combines deep learning architectures like LSTM and CNN. Extraction and use of DWT features are required for the analysis of images.

From the literature it is acknowledged that basic CNN models have difficulties managing rotated, tilted, or abnormal image orientations. The combined Deep-Net model that is proposed intends to overcome the difficulty and enhance performance in identifying wood faults.

IV. METHODOLOGY

The proposed experiment is performed on a dataset of wood texture i.e. Large Scale Image Dataset of Wood Surface Defects [22]. This includes different kinds of wood surface defects which can be normally seen in wood surfaces. The dataset contains the 4000 images with 8 different classes namely: Quartzity, Live_Knot, Marrow, resin, Dead_Knot, knot_with_crack, Knot_missing and Crack. The dataset contains the annotation file for the classification, which is used for dataset creation for the proposed experimentation.

For the experimented dataset applied the different generalized pre-processing techniques and further directional information of images is extracted using DWT and with help of Deep-Net model (CNN and LSTM) classified the different defects present in the dataset.

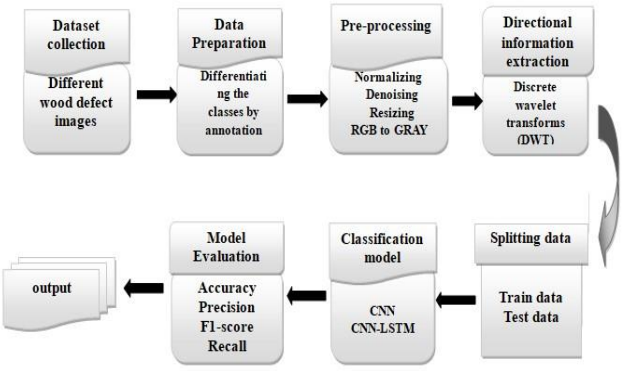

Figure 1. Flow diagram of the proposed methodology

The Figure 1 illustrates the comprehensive workflow of the proposed project. The initial phase involves gathering a dataset containing various wood defect images. This dataset is obtained from a large-scale wood defect detection dataset, accompanied by an annotation file. Following this, different classes are created through data preparation using the dataset and its annotation file.

Subsequently, the prepared data undergoes generalized preprocessing techniques to ensure uniformity and enhance the quality of the images. In the subsequent step, directional information is computed for each image utilizing Discrete Wavelet Transform (DWT) techniques. Specifically, the four different directional coefficients of each image are extracted and saved for further processing.

The data is then split into training and testing sets to facilitate model training and evaluation. For the classification task, a Deep-Net model, a combination of Convolutional Neural Network (CNN) and Long Short-Term Memory (LSTM) models, is employed. The model's performance and effectiveness are evaluated, and the results of the model evaluation are documented comprehensively.

Following sub-sections encapsulates a detailed summary of each of these steps, providing an organized overview of the methodology.

4.1. Data collection

The benchmark dataset considered for the study is downloaded from the Kaggle [22].Original dataset have high resolution images captured with special camera taking up roughly 12 megabytes (MB) of storage space is required for each image. The dataset contains the total of 4000 images of different wood defects and also it's having the Bounding Boxes - YOLO Format which consists the annotation file. Each image in the dataset is of size 2800x1024.The images describes the different wood surface defects of 8 different types, namely: Quartzity, Live_Knot, Marrow, resin, Dead_Knot, knot_with_crack, Knot_missing and Crack. Detail about dataset is given in the Table 1. Sample images of each class from the dataset are shown in the Figure 2.

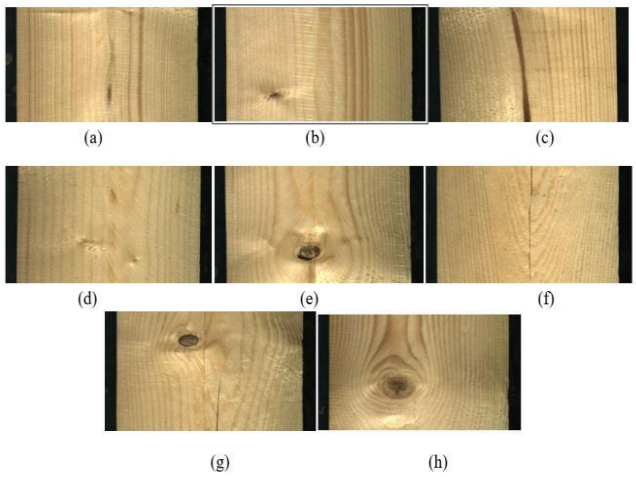

Figure 2. Sample images of all classes images from the dataset Large Scale Image Dataset of Wood Surface Defects [22], (a) Quartzity (b) Live_Knot (c) Marrow (d) resin (e) Dead_Knot (f) Crack (g) knot_with_crack (h) Knot_missing

4.2. Data preparation

From the set of 4000 images of 8 classes and annotation file that is available in kaggle, for the proposed work authors considered the images which are belong to 6 different classes. Total 493 images are taken for the proposed work because many of the images don't have the proper annotation and many of the images are having the combination of two or more defects in one image. Six classes out of eight classes are considered for the study because two classes having images which are very low in count.

Finally, 493 images separately and annotation file of these images separately formed the 6 different classes. Now the Proposed experimented dataset is having the 493 images with 6 different classes that are displayed in the Table 2.

The Table 1 and 2 describe the in-depth overview of the datasets before preparation and after preparation.

Table1. Description of the Large Scale Image Dataset of Wood Surface Defects dataset [22].

Original dataset	
Parameters	***Values***
Number of images	4000
Number of classes	8 (annotation file)
Image size	2800x1024
Dataset size	3.09 GB
Image format	RGB JPG

Table2. Description of dataset considered for the proposed experimentation.

New prepared dataset	
Parameters	***Values***
Number of images	493
Number of classes	6
Image size	2800x1024
Dataset size	389 MB
Image format	RGB JPG

4.3. Data pre-processing

Preprocessing is an essential stage in processes for data analysis and machine learning. In order to make unprocessed data suitable for additional analysis, modeling, or visualization, it must be prepared and cleaned. The main pre-processing procedures are as follows.

- Resize the Image: The image is resized to a fixed size of 128x128 pixels.
- Convert to Grayscale: The resized image is converted from its original representation (RGB) to greyscale.
- Denoising: function is used to perform denoising on the greyscale image. Denoising helps reduce noise and artifacts in the image, resulting in a cleaner and smoother image.
- Normalization: To normalise the denoised image, divide each pixel value by 255.0. In this stage, the pixel values are scaled to lie between 0 and 1.

4.4. Feature extraction using discrete wavelength transform

For the experiment Discrete Wavelet Transform (DWT) is applied to an image using the Haar wavelet, the transformed image is represented by a set of coefficients. These coefficients are categorized into 4 components details: approximation, horizontal, vertical, and diagonal. Each of these components captures different aspects of the image's frequency content and structure.

- By using DWT offers a multi resolution representation of the image that divides it into many granularities. This enables the analysis of flaws at many scales, ranging from minute details to vast patterns.DWT helps in localizing defects within an image. By decomposing the signal into different frequency components.
- DWT extracts pertinent aspects that can help in defect detection. It is simpler to distinguish between normal and faulty areas when different frequency components that were collected by DWT are used to depict the distinctive characteristics of defects.

Following are the different coefficients which are used:

- Approximation Coefficient (cA):
  The low-frequency components of the image are represented by the approximation coefficient. It has a lower resolution "averaged" version of the original image.
- Horizontal Detail Coefficient (cH):
  The image's horizontal edges and high-frequency elements are described by the horizontal detail coefficient.
- Vertical Detail Coefficient (cV):
  The image's vertical edges and high-frequency elements are described by the vertical detail coefficient.
- Diagonal Detail Coefficient (cD):

The diagonal detail coefficient records the image's high-frequency elements and diagonal edges.

The Figure 3 shows the sample images of the class Dead_Knot after applying the DWT directional feature extraction.

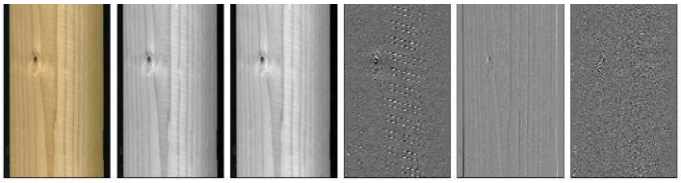

(a) (b) (c) (d) (e) (f)

Figure 3. Images of the Dead_Knot class after applying one level DWT (a) Original image (b) Converted Grayscale image (c) Approximation image (d) Horizontal detail image (e) Vertical detail image (f) Diagonal detail image.

4.4.1 Interpretation and Applications

The Haar wavelet coefficients obtained from the DWT are powerful tools for analyzing and processing images [23]. By analyzing the characteristics of these coefficients, one can gain insights into the image's various frequency components, details, and structures. These coefficients find applications in various fields, including image compression, denoising, feature extraction, and image enhancement. Depending on the specific application, different combinations of these coefficients can be used to achieve the desired outcomes.

4.5. Deep-Net (CNN-LSTM) model for classification

When dealing with data sequences, convolutional neural networks (CNNs) and long short-term memory (LSTM) networks can be used to classify the data. A deep learning architecture called Deep-Net (CNN-LSTM) Model was created to analyze visual sequences and predict outcomes. It effectively captures both spatial and temporal elements within sequential image data by utilizing Convolutional Neural Networks (CNNs) and Long Short-Term Memory (LSTM) layers.

4.5.1 Architecture Overview:

1. CNN Feature Extraction: The model's initial layers consist of 2D convolutional layers (Conv2D) with Rectified Linear Unit (ReLU) activation functions. These layers extract spatial features from each frame of the input sequence. Max-pooling layers are employed to downsample the features while preserving important information.

2. LSTM Temporal Modeling: The output from the CNN layers is then fed into LSTM layers, which are specialized for capturing temporal patterns in sequential data. The LSTM layers enable the model to learn dependencies between frames over time.

3. Dense Layers for Classification: Following the LSTM layers, dense (fully connected) layers are introduced to perform classification tasks. These layers process the output from the LSTM layers and generate predictions based on learned features. Dropout layers are used for regularization to prevent over fitting.

4. Sigmoid Activation for Multi-Label Classification: The final dense layer employs a sigmoid activation function, enabling the model to make multi-label predictions. Each unit in this layer corresponds to a specific class label, and the sigmoid activation produces a binary output for each class.

The figure 4 shows the created Deep-Net model for the proposed experimentation.

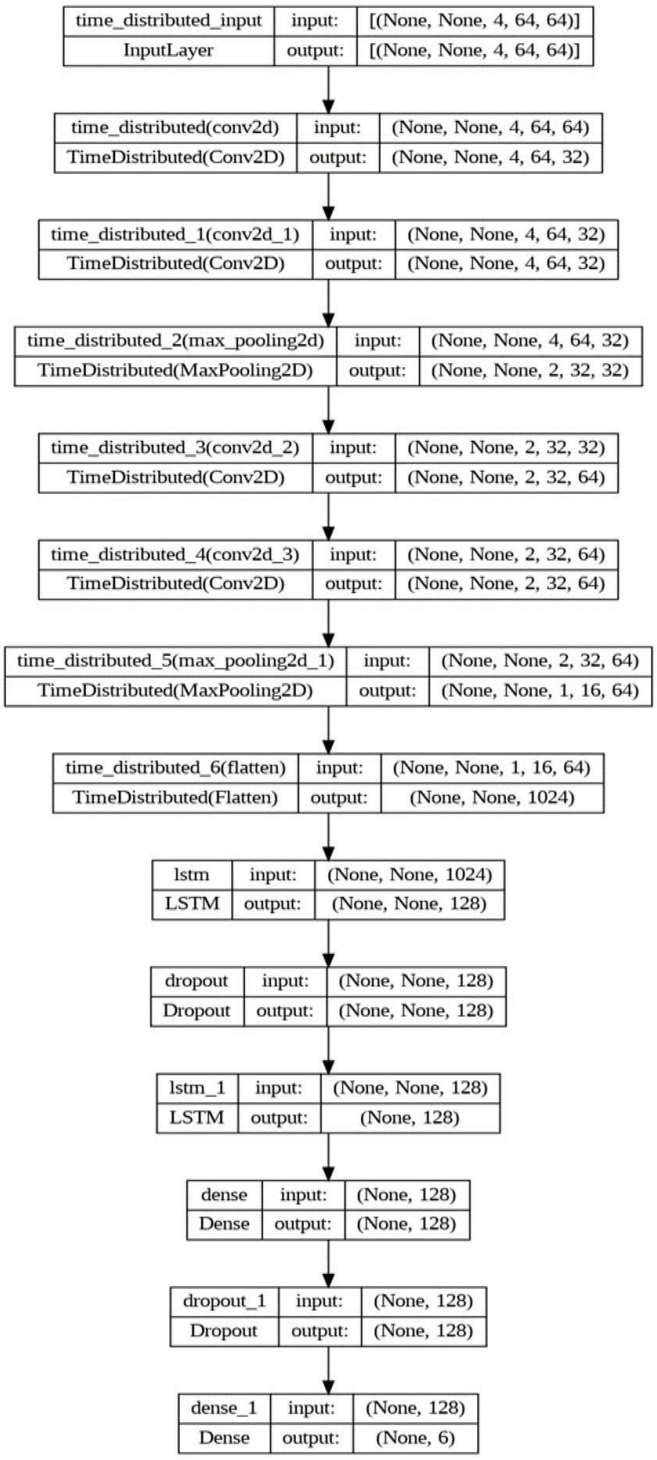

Figure 4. Deep-Net model: CNN with LSTM model

V. EXPERIMENTAL RESULT

The experimental setup utilized a 64-bit version of Windows 10, running on an Intel Core i3 processor clocked at 2.40GHz, coupled with 4GB of RAM. Python modules, including scikit-learn, matplotlib, and TensorFlow, were instrumental in constructing the model.

5.1 Data interpretation and splitting the data

The Figure 5 shows the images per class in the dataset which is used for the proposed study.

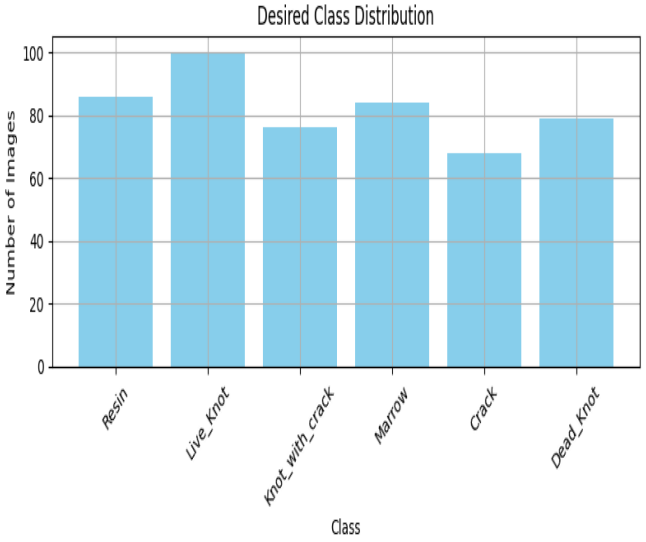

Figure 5. Image distribution in each class

Figure 5 represents the distribution of images per class within the dataset employed for this study. The following classes were included:

- "Resin"
- "Live_Knot"
- "Knot_with_crack"
- "Marrow"
- "Crack"
- "Dead_Knot"

The graph visually depicts the distribution of images across these classes, providing insights into the dataset's class balance or imbalance.

Figure 6 illustrates the dataset split into training and test sets following a 70:30 ratio. The graph represents the allocation of data for training and validation purposes.

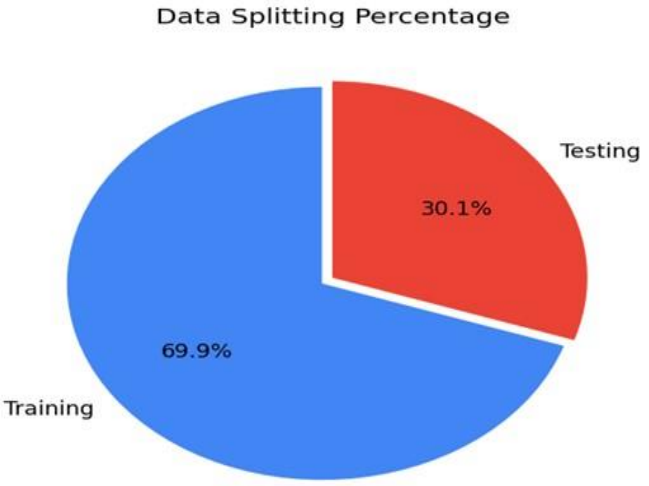

Figure 6. Training, testing ratio graph

• Test Size: 0.3 indicates a 30% allocation for the validation set, leaving 70% for the training set.

This division ensures that a substantial portion of the dataset is reserved for training the model while allowing a

sizable portion for validation to assess the model's performance without overfitting.

The chosen split ratio of 70:30 strikes a balance between model training and validation, ensuring adequate data for both purposes. The division of data into training and test sets at a 70:30 ratio facilitates robust model development and evaluation. This allocation strategy enables the model to learn from a substantial amount of data while ensuring an independent validation subset for accurate performance assessment.

5.2 Results and Discussion

Section provides a summary of the numerical outcomes, trends observedand graphical representations during experiment. The Figures 7 and 8 reports the accuracy scores or relevant metrics obtained from each experimental configuration from the different epoch ranges from 0 to 125. This provides a straightforward comparison of how the model's performance changed with varying epochs.

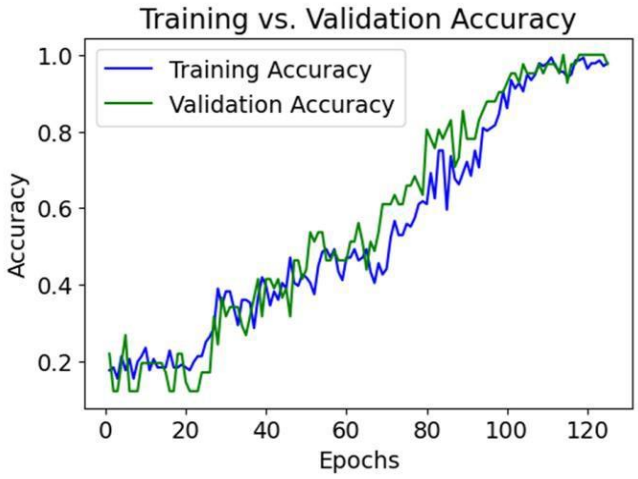

Figure 7. Accuracy of training and validation for different values of epochs

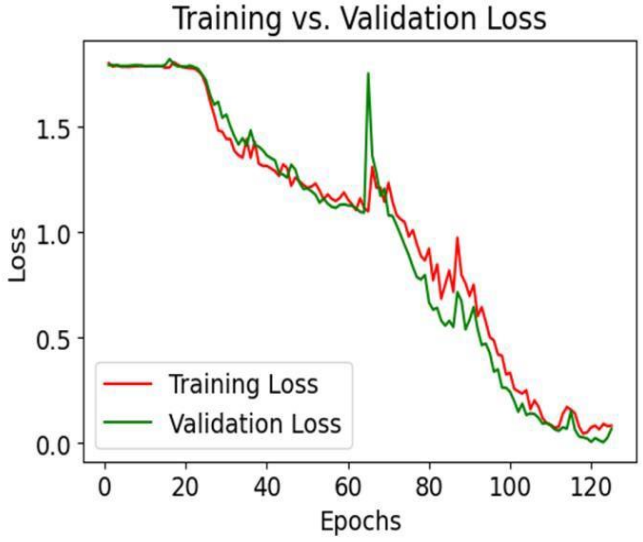

Figure 8. Loss of training and validation for different values of epochs

The accuracy and loss of a Deep-Net model changeover the course of training and validation, as shown in figures 7 and 8. It illustrates how accuracy typically increases and loss typically decreases as the model gains knowledge from the training data. This demonstrates how the model's accuracy and capacity for event prediction grow as it is taught.

From Figures 7 and 8, it's evident that the experiment utilized an epoch value of 125. Throughout the epochs, a noticeable trend in accuracy is observed, steadily increasing from 0 up to the 100th iteration. However, beyond the 100th iteration, the model's accuracy plateaus, remaining constant thereafter.

Figure 9 specifically presents the accuracy trends for the final 20 epochs of the experiment, offering a closer examination of the model's performance during this concluding phase.

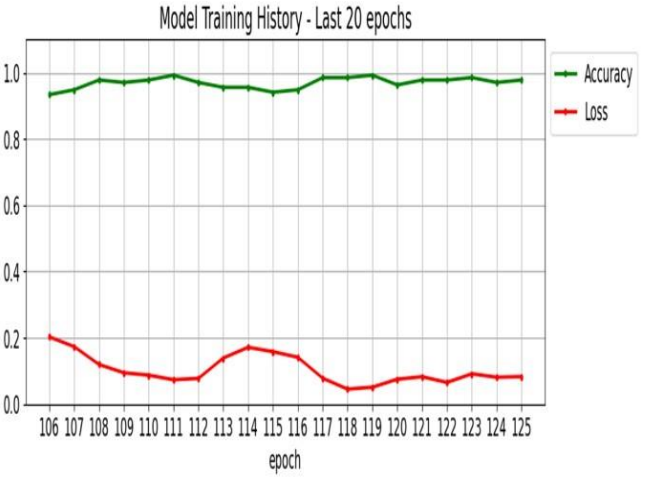

Figure 9. Model training history of last 20 epochs

Tables 3 and 4 furnish a detailed breakdown of the classification performance metrics for distinct classes in the model's predictions. These metrics encompass Precision, Recall, and F1-score, providing a comprehensive assessment of the model's ability to differentiate between classes.

A conclusion section must be included and should indicate clearly the advantages, limitations, and possible applications of the paper. Although a conclusion may review the main points of the paper, do not replicate the abstract as the conclusion. A conclusion might elaborate on the importance of the work or suggest applications and extensions.

Table 3. Classification table for train set

Class	Precision	Recall	f1-score
Live_Knot	1.00	1.00	1.00
Marrow	1.00	0.96	0.98
Resin	0.95	1.00	0.97
Dead_Knot	0.96	1.00	0.98
Knot_with_crack	1.00	1.00	1.00

Crack	1.00	0.95	0.91

Table 4: Classification table for test set

Class	Precision	Recall	f1-score
Live_Knot	1.00	1.00	1.00
Marrow	1.00	1.00	1.00
Resin	0.86	1.00	0.92
Dead_Knot	1.00	1.00	1.00
Knot_with_crack	1.00	1.00	1.00
Crack	1.00	0.83	0.91

From the Table 3 and 4 it is observed that the table provides a comprehensive overview of the classification metrics for each class in our model's predictions. The metrics include Precision, Recall, and F1-score. These metrics collectively illuminate the model's performance in distinguishing between different classes.
The model's overall performance appears to be strong, as indicated by the consistently high precision, recall, and F1-scores across various classes. However, the variation s in metrics for certain classes, such as "Marrow" and "Crack," suggests potential areas for improvement.

The Table 5 below shows the model performance metrics of Deep-Net model for the proposed experiment.

Table 5. Model Performance Metrics table for train & test set

Model Performance Metrics	Accuracy in %
Train Accuracy	98.52
Train Loss	04.52
Test Accuracy	97.56
Test Loss	06.77

The Table 5 presents the model's performance metrics for both the training and testing sets. The training accuracy stands at 98.52%, signifying the model's correct prediction of nearly 98.52% of the training dataset. The associated training loss is 4.52, indicating minimal error or discrepancy in predictions during the training phase.
On the other hand, the model achieved an accuracy of 97.56% on the separate testing dataset, demonstrating its ability to accurately predict around 97.56% of the unseen test data. The corresponding test loss is 6.77%, suggesting a relatively low level of error in predictions on the unseen test data.
In essence, these metrics highlight the model's strong performance on both the data it learned from and its ability to generalize well to new, unseen data, showcasing high accuracy and comparatively low error rates.

In Figures 10 and 11, the displayed confusion matrix utilizes the "Normalized" format, presenting values as percentages or proportions. This format helps elucidate the distribution of prediction errors across various classes, even in the presence of imbalanced class counts. It offers a clearer insight into how mistakes in predictions are distributed among different classes.
On the other hand, the "Class Count" Confusion Matrix showcases values based on the actual count of instances within each class. This format facilitates a direct comparison of performance across classes by explicitly illustrating the number of accurate and erroneous forecasts for each class. It provides a more tangible understanding of the accuracy and error distribution among different classes, enabling a direct comparison of the model's performance across diverse categories.

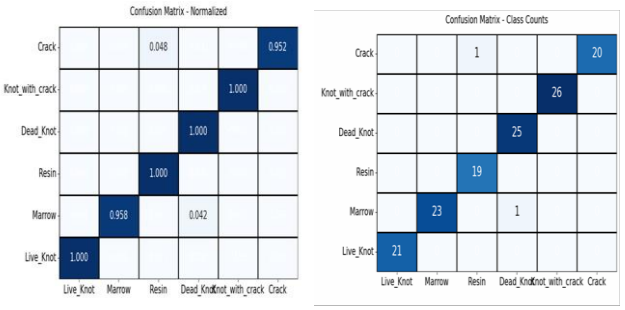

(a) Normalized **(b) class count**

Figure 10. Confusion matrix for normalized and class count for training set

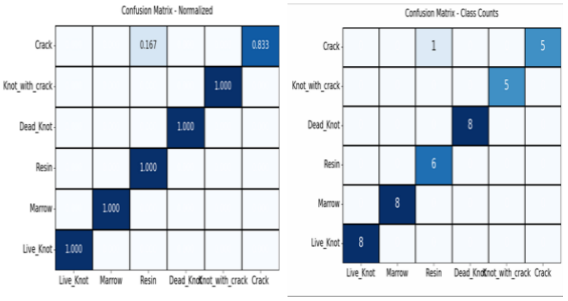

(a) Normalized **(b) class_count Figure 11.**
Confusion matrix for normalized and class count for test set

Figures 10 and 11 exhibit that the Deep-Net model accurately predicts the classes selected for the experiment. The model demonstrates proficiency in accurately identifying and classifying these specific classes, as indicated by the results depicted in the figures.
Figure 12 provides a graphical representation of precision, recall, and F1 scores for various classes, such as "Live_Knot," "Marrow," "Resin," "Dead_Knot," "Knot_With_Crack," and "Crack."
The precision score, depicting the accuracy of positive predictions, is graphically displayed for each class, illustrating the model's capability in correctly identifying instances of these classes.

Additionally, the graph showcases the recall score for each class, offering insights into the model's effectiveness in capturing positive occurrences accurately within each class. In essence, this graphical representation allows for a visual comparison of precision and recall scores across multiple classes, enabling a comprehensive understanding of the model's performance concerning these evaluation metrics for each specific class.
The graph displays the F1 score for each class, a statistic that balances recall and accuracy.

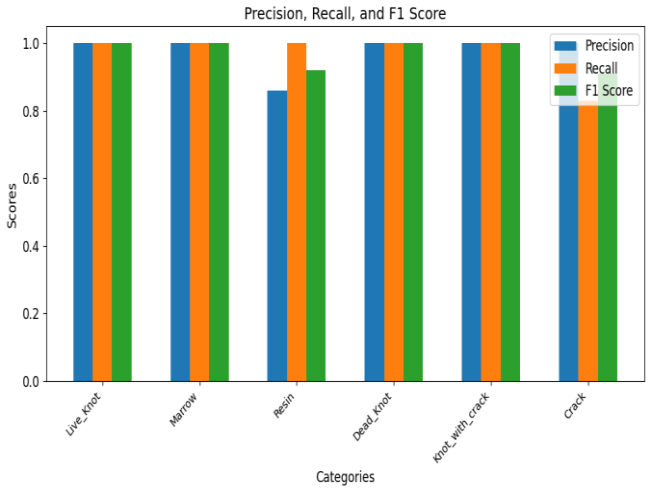

Figure 12. Precision, Recall, F1 score for classes of dataset.

Overall, the findings collectively indicate a strong performance of the Deep-Net model in identifying wood defect classes. While demonstrating high accuracy and proficiency in most classes, the model's performance aligns well with or surpasses existing state-of-the-art methodologies, affirming its efficacy in large-scale wood surface defect detection.

Table 5. Comparison of classification accuracy on the wood surface defect detection dataset between the proposed method and state-of-the-art-work.

Table 5 shows that the proposed experimental results with comparison of state-of-art work related to the dataset large scale wood surface defects detection [22].

From the table 5 it is observed that experimented model provide a greater categorization rate when evaluated using a cutting-edge methodology. The 98% accuracy is provided by Deep-Net model i.e. is by combining CNN and LSTM with DWT characteristics.

VI. CONCLUSION

Within this study, tackled the challenges of detecting defects in wood, with a primary focus on its applicability to automated wood surface defect detection. Our objective was to devise a cost-effective and robust algorithm that could seamlessly integrate into this machinery. To optimize affordability, we made the deliberate choice of utilizing grayscale-based features as opposed to color-based ones. The findings underscored the remarkable efficacy of proposed approach in recognizing wood defects. Notably, proposed method exhibited exceptional accuracy in defect recognition while maintaining commendable real-time performance.
In the context of identifying six distinct types of wood defects, Convolutional neural networks (CNN) and long short-term memory (LSTM) was combined and created Deep-Net model which delivered an impressive identification accuracy of 98% with DWT. This innovative fusion demonstrates its potential to serve as a powerful tool in significantly enhancing the detection of surface defects in solid wood surface. In future the proposed experiment can be continued with all 8 classes. And using the advanced pre processing techniques can classify more number of defects presented in wood surface.

ACKNOWLEDGEMENT

Authors are thankful to the reviewers for suggestions and constructive criticism that helped to enhance the quality of the manuscript.

REFERENCES

[1]. Wang, L., Qi, W., Wu, J., &Hou, W. (2007, August). Recognizing the patterns of wood inner defects based on wavelet neural networks. In 2007 IEEE International Conference on Automation and Logistics (pp. 1719-1724). IEEE.10.1109/ICAL.2007.4338850

[2]. Du, X., Li, J., Feng, H., & Chen, S. (2018). Image reconstruction of internal defects in wood based on segmented propagation rays of stress waves. Applied Sciences, 8(10), 1778.https://doi.org/10.3390/app8101778

[3]. Peng, Z., Yue, L., & Xiao, N. (2016). Simultaneous wood defect and species detection with 3D laser scanning scheme. International Journal of Optics, 2016.https://doi.org/10.1155/2016/7049523

[4].Wang, Q., Liu, X. E., & Yang, S. (2020). Predicting density and moisture content of Populusxiangchengensis and Phyllostachysedulis using the X-ray computed tomography

Sl. No.	Work in literature	Methodology	Classification Accuracyin%
01	Gonzalo A. Ruz [20]	Fuzzy min max neural network	94.4%
02	Augustas Urbonas [21]	ResNet152 neural network	96.1%
03	**Proposed method**	**DWT CNN+LSTM**	**98%**

technique. Forest Products Journal, 70(2), 193-199.**https://doi.org/10.13073/FPJ-D-20-00001**

[5] França, F. J. N., França, T. S. F. A., Seale, R. D., &Shmulsky, R. (2020). Nondestructive evaluation of 2 by 8 and 2 by 10 southern pine dimensional lumber. Forest Products Journal, 70(1), 79-87.**https://doi.org/10.13073/FPJ-D-19-00051**

[6] Ke, Z. N., Zhao, Q. J., Huang, C. H., Ai, P., & Yi, J. G. (2016, July). Detection of wood surface defects based on particle swarm-genetic hybrid algorithm. In 2016 International Conference on Audio, Language and Image Processing (ICALIP) (pp. 375-379). IEEE.10.1109/ICALIP.2016.7846635

[7] He, T., Liu, Y., Yu, Y., Zhao, Q., & Hu, Z. (2020). Application of deep convolutional neural network on feature extraction and detection of wood defects. Measurement, 152, 107357.**https://doi.org/10.1016/**j.measurement.2019.107357

[8] Mahmood, T., Ashraf, R., & Faisal, C. N. (2022). An efficient scheme for the detection of defective parts in fabric images using image processing. The Journal of The Textile Institute, 1-9. https://doi.org/10.1080/00405000.2022.2105114

[9] Bhusnurmath, R. A., &Doddamani, S. (2023, June). Bark Texture Classification Using Deep Transfer Learning. In International Conference on Multi-disciplinary Trends in Artificial Intelligence (pp. 407-420). Cham: Springer Nature Switzerland. https://doi.org/10.1007/978-3-031-36402-0_38

[10] Hiremath, P. S., &Bhusnurmath, R. A. (2017). Multiresolution LDBP descriptors for texture classification using anisotropic diffusion with an application to wood texture analysis. Pattern Recognition Letters, 89, 8-17. https://doi.org/10.1016/j.patrec.2017.01.015.

[11] Gao, M., Wang, F., Liu, J., Song, P., Chen, J., Yang, H., & Yue, H. (2022). Estimation of the convolutional neural network with attention mechanism and transfer learning on wood knot defect classification. Journal of Applied Physics, 131(23).https://doi.org/10.1063/5.0087060

[12] Sun, P. A. (2022). Wood quality defect detection based on deep learning and multicriteria framework. Mathematical Problems in Engineering, 2022, 1-9.https://doi.org/10.1155/2022/4878090

[13] Celik, Y., Guney, S., &Dengiz, B. (2022, July). Applications of deep learning techniques to wood anomaly detection. In International Conference on Management Science and Engineering Management (pp. 379-387). Cham: Springer International Publishing.https://doi.org/10.1007/978-3-031-10388-9_27

[14] Li, S., Li, D., & Yuan, W. (2019). Wood defect classification based on two-dimensional histogram constituted by LBP and local binary differential excitation pattern. IEEE Access, 7, 145829-145842.10.1109/ACCESS.2019.2945355

[15] Ji, X., Guo, H., & Hu, M. (2019, September). Features extraction and classification of wood defect based on HU invariant moment and wavelet moment and BP neural network. In Proceedings of the 12th International Symposium on Visual Information Communication and Interaction (pp. 1-5).https://doi.org/10.1145/3356422.3356459

[16] Hwang, S. W., Lee, T., Kim, H., Chung, H., Choi, J. G., & Yeo, H. (2022). Classification of wood knots using artificial neural networks with texture and local feature-based image descriptors. Holzforschung, 76(1), 1-13.https://doi.org/10.1515/hf-2021-0051

[17] Gao, M., Qi, D., Mu, H., & Chen, J. (2021). A transfer residual neural network based on ResNet-34 for detection of wood knot defects. Forests, 12(2), 212.**https://doi.org/10.3390/f12020212**

[18] Mousavi, M., &Gandomi, A. H. (2021). Wood hole-damage detection and classification via contact ultrasonic testing. Construction and Building Materials, 307, 124999.https://doi.org/10.1016/j.

[19] Yang, Y., Wang, H., Jiang, D., & Hu, Z. (2021). Surface detection of solid wood defects based on SSD improved with ResNet. Forests, 12(10), 1419. **https://doi.org/10.3390/f12101419**

[20] Ruz, G. A., Estevez, P. A., & Perez, C. A. (2005). A neurofuzzy color image segmentation method for wood surface defect detection. Forest products journal, 55(4), 52-58.

[21] Urbonas, A., Raudonis, V., Maskeliūnas, R., &Damaševičius, R. (2019). Automated

Int. J. Advanced Networking and Applications
Volume: 15 Issue: 04 Pages:100-200 (2023) ISSN: 0975-0290 (Special Issue – ASCIS 2023)

identification of wood veneer surface defects using faster region-based convolutional neural network with data augmentation and transfer learning. Applied Sciences, 9(22), 4898.**https://doi.org/10.3390/app9224898**

[22] https://www.kaggle.com/datasets/nomihsa965/large-scale-image-dataset-of-wood-surface-defects

[23] Hiremath, P. S., &Bhusnurmath, R. A. (2017). Industrial applications of colour texture classification based on anisotropic diffusion. In Recent Trends in Image Processing and Pattern Recognition: First International Conference, RTIP2R 2016, Bidar, India, December 16–17, 2016, Revised Selected Papers 1 (pp. 293-304). Springer Singapore.https://doi.org/10.1007/978-981-10-4859-3_27